Int J Physiol Pathophysiol Pharmacol 2009;1:15-24
www.ijppp.org/IJPPP812001

Original Article

Amyloid-beta alters trafficking of internalized acetylcholinesterase and dextran

William Hu[1,2‡], Noah W. Gray[2*], Stephen Brimijoin[1,2]

[1]Department of Molecular Pharmacology, Mayo Medical School, Rochester MN; [2]Molecular Neuroscience Program, Mayo Foundation, Rochester MN

Received December 18, 2008; accepted December 22, 2008; available online January 1, 2009

Abstract: Amyloid-beta (Aβ), the main peptide constituent of senile plaques, is a suspected pathogenic mediator in Alzheimer's Disease (AD). Plaques also contain acetylcholinesterase (AChE), which may promote Aβ toxicity. We previously found that Aβ increased AChE levels in neuron-like N1E.115 neuroblastoma cells by reducing AChE degradation and surface shedding. Here we show that Aβ also alters the intracellular fate of surface AChE. When surface AChE was tagged with FITC-conjugated Fasciculin II (FasII), fluorescence gradually accumulated in intracellular particles. In the presence of extracellular Aβ this accumulation increased and shifted from the juxtanuclear zone to more peripheral cytoplasm. The cytoplasmic FasII-positive structures were positive for Lysosomal-Associated Membrane Protein 1, identifying them as late endosomes and early lysosomes. Thus, surface AChE trafficked into the lysosomal compartment, but further transport was impaired. Aβ also affected the transport or disposition of fluorescent dextran, an index of pinocytosis, and caused a 60% increase in intracellular accumulation similar to the lysosomotropic effects of chloroquine. On the other hand, Aβ caused no apparent changes in clathrin- and caveolae-mediated endocytosis. Overall it appears that selective alteration of endocytic mechanisms and an accumulation of organelles containing improperly processed substrates might contribute to the neuronal damage associated with age and disease-related accumulation of neurotoxic Aβ in the human brain.

Key Words: Alzheimer's disease, lysosome, endocytosis, pinocytosis

Introduction

In Alzheimer's Disease (AD), amyloid beta (Aβ) peptides aggregate to form insoluble neurotoxic fibrils that promote disease progression [1, 2]. Multiple lines of evidence point to disturbances of internalization and intracellular turnover as harbingers of AD pathology. For example, enlarged early endosomes in brains from patients with AD and Down's syndrome are suggestive of altered endocytosis [3, 4]. A similar interpretation can be placed on the in vitro demonstration that Aβ accelerates the cellular secretion of an internalized dye known as MTT, or 3-(4,5-dimethylthiazol-2-yl)-2,5-diphenyltetrazolium bromide [5-7]. These findings are important because an altered balance of endocytosis and secretion could also promote AD progression by increasing the levels of Aβ in cells, along with surface molecules that enhance the cytotoxicity of this peptide [3, 5, 8, 9].

Acetylcholinesterase (AChE, EC 3.1.1.7) is one surface molecule that increases Aβ toxicity in neuronal cell culture by accelerating fibril formation [10, 11]. In a mouse model of AD, an increased expression of AChE is also associated with early formation of Aβ plaques

‡Present Address: University of Pennsylvania (William.Hu@uphs.upenn.edu)

*Present Address: Nature Neuroscience (n.gray@natureny.com)

in cerebral cortex and hippocampus [12]. There is other evidence that AChE and Aβ may interact in a pathogenically significant fashion. We recently showed that Aβ slowed the overall degradation of AChE in neuroblastoma cells by elevating lysosomal pH and by inhibiting the surface shedding of this protein [13]. A critical step in the intracellular degradation of surface AChE is internalization and intracellular transport. Although relatively little is known about the physiology of this step, fasciculin II (FasII), a potent AChE inhibitor derived from snake venom, has proved useful in visualizing surface AChE in Xenopus muscle cells [14, 15]. Here we employed fluorescent FasII as a probe for surface AChE in order to investigate the internalization of this enzyme in the presence and absence of Aβ.

Materials and Methods

Aβ1-42 and Aβ25-35 peptides (US Peptides, Rancho Cucamonga, CA) were reconstituted in dimethylsulfoxide (DMSO) at 10 mg/ml and stored at –20°C. Before addition to cultures, Aβ1-42 (but not Aβ25-35) was incubated at 37°C for 3 days to promote aggregation. Dulbeco's modified Eagle's medium (DMEM) and fetal bovine serum (FBS) were purchased from Invitrogen (Carlsbad, California). FasII, a 61-amino acid α-neurotoxin from the venom of the African green mamba, was purchased from Alomone Laboratories (Jerusalem, Israel). Tetramethyl-rhodamine (FluoReporter), FITC-Transferrin (Trf), FITC-cholera toxin B (CTB), FITC-dextran, and Anti-Fade were from Molecular Probes (Eugene, OR). Monoclonal FITC-conjugated Lysosome Associated Membrane Protein-1 (LAMP-1) antibody was from Santa Cruz Biotechnology. "Ultrapure" formaldehyde was obtained from Tousimis (Rockville, MD). Centricon microconcentrators were from Millipore (Bedford, MA). Other materials were purchased from Sigma-Aldrich (St. Louis, MO).

Cell culture

All studies were performed on wild type N1E.115 neuroblastoma cells, which were grown on 20 x 20 mm glass coverslips to facilitate microscopic analysis. Cells were initially maintained in 10% CO_2 at 37°C in DMEM with 2.5% fetal bovine serum, 100 units/ml penicillin, and 100 μg/ml streptomycin. After 24 h, this medium was replaced with serum-free medium containing 1 μM Aβ or DMSO vehicle (final concentration ≈ 0.01%) for exposures of varying duration (typically 24 h).

AChE sorting after synthesis

To track AChE membrane insertion and sorting we examined the reappearance of AChE activity after irreversible inhibition of cellular cholinesterases by di-isopropylfluorophosphate (DFP, 10^{-7} M). Cells were treated with vehicle or Aβ for 22 h, followed by DFP for 15 min. Inhibitor was then removed by three 5-min washes with serum-free DMEM, and cells were returned to normal conditions with 2 mL of medium. Exactly 75 min later, 20 μL of 100 μM echothiophate or water was added and cells were kept for 15 min at 4°C. Under these conditions, echothiophate is excluded from the cell and selectively "labels" surface AChE by inhibiting enzyme activity [16]. Treated cells were lysed by freeze-thawing in 200 μl of 10 mM Tris-HCl (pH 7.4), 1 M NaCl, 1% Triton X-100, followed by centrifugation (10,000 x g, 10 min). AChE activity in 50-μL aliquots of the supernatants was assayed by measuring release of ^{3}H acetate from ^{3}H acetylcholine over a 90 min period [17]. Reactions were conducted at room temperature in the presence of ethopropazine (10^{-4} M) to suppress butyrylcholinesterase activity.

Fluorescence-labeling of AChE with FasII

For selective fluorescent labeling of surface AChE, 14 μg of FasII in 210 μl water with 10 μmol $NaHCO_3$ was conjugated with 100 μg of tetramethylrhodamine in 10 μl of DMSO for 1 h at room temperature. Unconjugated label was removed by centrifugation in a 3 kD-Centricon filter for 10 min at 10,000 g. The specificity of the rhodamine-conjugated toxin and its ability to bind AChE under various conditions were tested as described under Results.

Measures of internalization

To study internalization of FasII-labeled AChE without uptake of free FasII, cells were incubated with 10 nM rhodamine-conjugated toxin for 15 min at 4°C and then washed extensively before raising temperature to 37°C. After 24 h, cells were incubated in medium containing transferrin (Trf), cholera

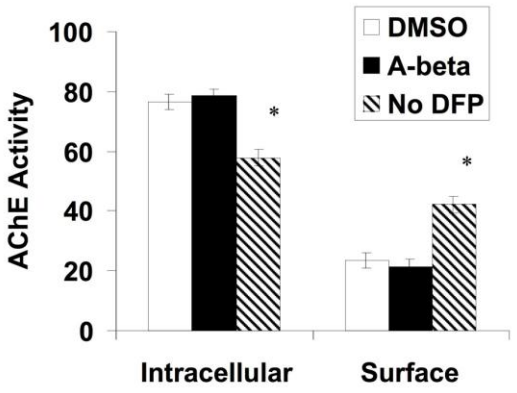

Figure 1. Effects of Ab on sorting of newly synthesized AChE. Cells were exposed to 1 μM Ab or 1% DMSO vehicle. Recovered AChE activity after DFP-inhibition was analyzed by echothiophate. Echothiophate-resistant AChE was considered to represent an intracellular pool; sensitive AChE was considered to represent a surface pool (values sum to 100%). Means and standard errors are shown. * Values from DMSO and Ab groups do not differ from each other but both differ significantly from no-DFP control ($p < 0.001$).

toxin subunit B (CTB), or dextran as markers of clathrin-mediated, caveolae-mediated, and fluid phase endocytosis, respectively. To test the first two endocytic pathways, cells were kept in 50 nM FITC-Trf for 15 min or 50 ng/mL FITC-CTB for 30 min. After Trf exposure, cells were also acid-stripped (pH 3.5) to remove surface Trf before further processing. To test fluid phase internalization, or pinocytosis, 25 μM FITC-dextran was presented for uptake for 2 h. At the conclusion of some experiments, cells were permeabilized and lysosomes were identified by FITC-conjugated monoclonal antibodies against LAMP-1 (5 μg/mL) applied at 37°C for 1 h [18].

Aβ and endocytosis

To test effects of Aβ on AChE internalization, existing surface AChE was first labeled with FasII as described above and then exposed to vehicle or Aβ for 44 h, approximately the internalization half-life of AChE [19, 20]. This timing allowed optimal visualization of internalized FasII. In a second set of experiments, cells were pre-treated with Aβ or vehicle for 22 h before FasII exposure and were returned to the previous treatment conditions for an additional 44 h after the brief labeling. This paradigm permitted the tracking of AChE inserted into the cell surface under control or treatment conditions. Two independent, treatment-blind observers evaluated the captured images and assigned each cell to one of four categories: 1) unlabeled, 2) with one or two FasII-vesicles, 3) with multiple fused FasII bodies, or 4) with FasII vesicles widely dispersed in cytoplasm.

To analyze effects of Aβ on other forms of endocytosis, fluorescent Trf, CTB, and dextran were presented briefly for binding and uptake after Aβ-pretreatment, since these markers have relatively rapid endocytic kinetics. Images were evaluated under blinded conditions using IPLab software (Scanalytics, Fairfax, VA), and total intracellular fluorescence was calculated as the product of average cellular intensity and cell area.

Laser scanning confocal microscopy

Cells were fixed in 3.3% "ultrapure" TEM formaldehyde for 15 min, washed in cold TBS and mounted on glass slides in 20 μL of Anti-Fade. For LAMP-1 immunocytochemistry cells were fixed and permeabilized before addition of antibodies. Images were obtained with a 63X objective (1.4 N.A.) on a Zeiss LSM 510 confocal microscope. A helium/neon laser at 568 nm and an argon/krypton laser at 488 nm were used for tetramethylrhodamine and FITC excitation, respectively. Images were optically sliced at 0.8-1.0 μm using LSM software. For unbiased comparisons, section thickness, laser power, contrast and brightness, and signal amplification were held constant for each pair of control and treatment conditions.

Statistical analysis

Unless otherwise specified, Student's t-test (run with StatView; SAS, Cary, NC) was used to analyze effects of treatment; p values < 0.5 were considered statistically significant.

Results

Aβ and AChE sorting after synthesis

Recovery of AChE activity after irreversible inhibition is an index of the generation of newly synthesized AChE molecules. To examine the fate of newly synthesized AChE en route to the plasma membrane, we used a

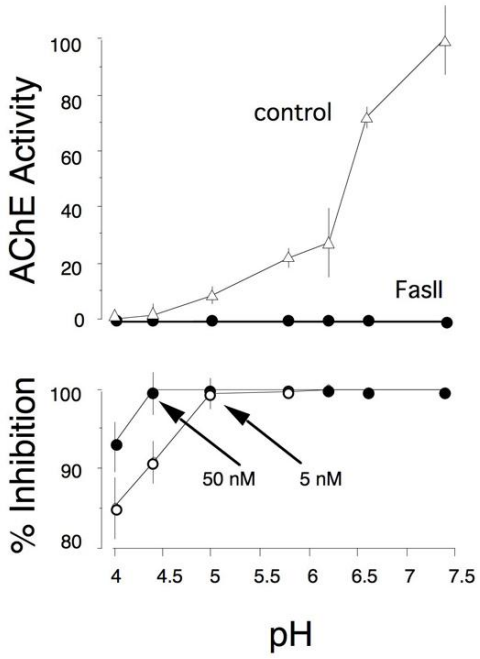

Figure 2. Effects of pH on AChE-FasII interaction. The proportion of AChE bound by FasII was determined by the percentage inhibition of AChE activity in mouse brain extracts tested at a variety of pH values. Reduced pH caused a powerful reduction in overall AChE activity (percent of mean value at pH 7.4) but minimal effects on inhibition by 5 nM or 50 nM FasII (which did not differ significantly from 100%).

sequence of DFP and echothiophate exposure. DFP was first applied to eliminate AChE activity irreversibly in all compartments and, after washout, 75 min were allowed for *de novo* enzyme synthesis. Echothiophate was then applied to inhibit membrane AChE, selectively and irreversibly (see Methods). In cells never exposed to DFP, 42 ± 3% of the AChE activity was echothiophate-sensitive and presumably located on the cell surface (**Figure 1**). After DFP exposure, a much smaller fraction of newly synthesized AChE was echothiophate sensitive, but the actual percentages in cells treated with Aβ (1 μM, 24 h) and vehicle (0.01% DMSO) were nearly the same (22 ± 2.4% and 23±2.5%, respectively). Aβ thus did not alter the apparent distribution of newly synthesized AChE between intracellular compartments and the cell surface.

FasII binding and internalization

AChE trafficking from the membrane was examined using the quasi-irreversible and selective inhibitory ligand, FasII. First, however, as high affinity AChE-FasII complexes depend on pH-sensitive hydrogen bonds, we tested FasII-mediated inhibition under acidic conditions like those in endosomes and lysosomes. As expected, the basal activity of AChE in mouse brain extracts declined sharply at low pH. Nonetheless it was clear that FasII inhibited the enzyme completely at pH 5 and above (**Figure 2**). Even at pH 4, a level associated with mature lysosomes, 5 nM FasII still inhibited by 85%, indicating that its affinity for AChE remained substantial. Furthermore, the surface binding of fluorescent FasII was saturable and was blocked by 0.5 mM BW284c51 (not shown). These results collectively supported the use of FasII as a specific probe for surface AChE migrating into endosomes.

To examine AChE internalization, N1E.115 cells were exposed to FasII in culture medium along with Aβ or its vehicle (see Methods) and cells were examined 44 h later. Vehicle-treated cells showed modest amounts of intracellular FasII, primarily localized in juxtanuclear particles strongly labeled by antibodies to the lysosomal marker, LAMP-1 (**Figure 3A & B**). Similar FasII- and LAMP-1-positive structures were noticeably more

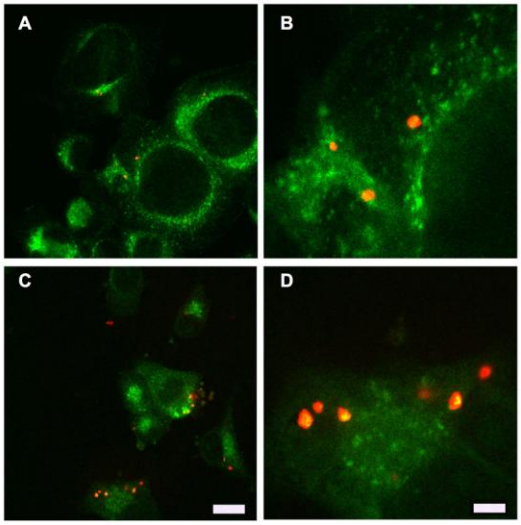

Figure 3. Fate of AChE labeled with FasII prior to treatment with DMSO or Aβ. Cells were co-stained for LAMP-1 (green). FasII (red) is less abundant and more perinuclear in DMSO (A) than Aβ (C) treated cells. B and D represent enlarged views of A and C, respectively. Scale bars represent 25 μm in A and C, and 6.25 μm in B and D.

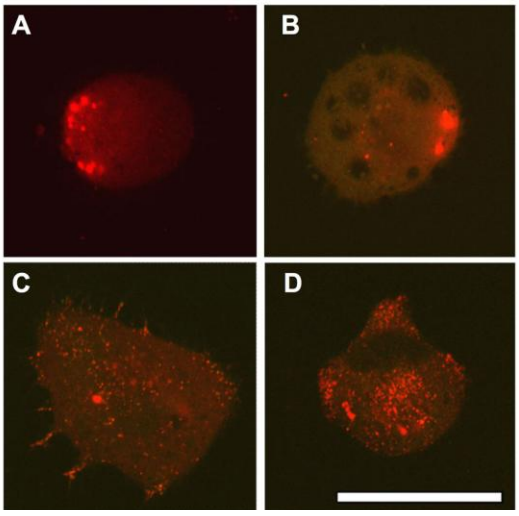

Figure 4. Typical appearance of FasII-containing cells after 44 h treatment with 1 μM Aβ or vehicle. Most FasII-containing cells after vehicle exposure had large juxtanuclear inclusions (A). Aβ treatment led to similar juxtanuclear inclusions (B), but also resulted in small and scattered cytoplasmic inclusion bodies in cells (C, D). Scale bar represents 50 μm.

abundant after Aβ-treatment (**Figure 3C & D**) but in this case the internalized fluorescence was found primarily in the peripheral cytoplasm.

We also tested a 66 h Aβ exposure in order to determine if the effect on AChE internalization and disposition would intensify over time. Cells were incubated with vehicle or Aβ for 22 h, exposed briefly to FasII, and then returned to their respective starting treatments for another 44 h (see Methods). Under these conditions, the proportion of FasII-positive cells was 45% higher after Aβ exposure (50 of 69) than after vehicle (29 of 58; $p < 0.001$). Juxtanuclear FasII inclusions were present in about half the cells of each group (**Figure 4 A & B**). In the Aβ-treated cells, however, a unique pattern of FasII distribution was observed independently by two treatment-blind observers. This was a "salt and pepper" scattering of fluorescence throughout the cytoplasm in bodies that were smaller than typical of mature endosomal or lysosomal structures (**Figure 4 C & D**).

This marked effect on FasII distribution might have reflected a generalized disturbance of endocytosis. To test that possibility we used a different fluorescence-tagged marker for each of three distinct pathways: fluorodextran (for pinocytosis); Trf (for clathrin mediated endocytosis); and CTB (for caveolae-mediated endocytosis). Among these markers, only fluorodextran was affected by a 24 h Aβ exposure, which induced a qualitatively apparent increase in intracellular accumulation (**Figure 5A, B**). This increase was most pronounced when dextran was in the media for the entire 24 h of Aβ treatment (**Figure 5C**). Quantitation of total intracellular fluorescence in 56 Aβ-treated cells (see Methods) demonstrated a 60% increase over the levels in 54 vehicle-treated controls (**Figure 5D**, $p < 0.001$). Intracellular fluorescence was above the control mean value (330 ± 17 arbitrary units) in 75% of the Aβ-treated cells (42 of 56) and was over 3 times control in 14% of those cells. These effects were highly significant by Chi-square analysis ($p < 0.00001$). The lysosomal inhibitor, chloroquine, 10 μM, also affected fluorodextran uptake. Like Aβ, it caused an 82% increase in mean fluorescence (**Figure 5E, F**, $p < 0.0001$). In contrast, a 24 h Aβ treatment had minimal effects on the uptake and accumulation of Trf, or CTB (data not shown).

AChE internalization and pinocytosis

Since FasII-AChE and fluorodextran were the only markers whose internalization was affected by Aβ, experiments were carried out to determine if internalized FasII and dextran shared similar intracellular compartments. A study of co-localization showed that internalized FasII was clearly not associated with Trf- or CTB-positive organelles (**Figure 6A, B**). Some FasII-containing vesicles were positive for dextran (**Figure 6C, D**), but they did not constitute a majority of either FasII- or dextran-containing vesicles, and they did not stain positive for Rab5 or Rab7 (data not shown). Thus, FasII did not stably co-localize with any of the other markers tested. The data are consistent, however, with the idea that dextran and AChE may share a common endocytic pathway that does not involve clathrin or caveolae.

Discussion

We previously reported that Aβ slowed AChE degradation in N1E.115 cells without altering

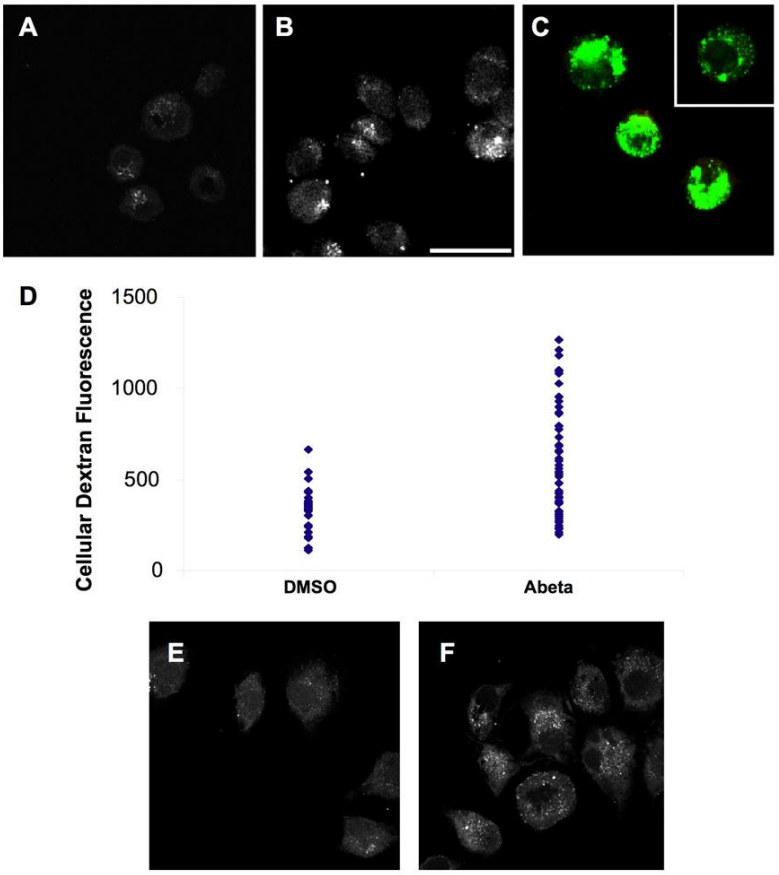

Figure 5. Effects of Aβ on endocytosis. A, B: 2-h dextran uptake in cells treated with DMSO (A) or Aβ (B). C: 24-h dextran accumulation DMSO (inset) and Aβ-treated cells. Scale bar represents 50 μm. D: Differential 24-h dextran accumulation in cells treated by DMSO and Aβ. Treatment with 10 μM chloroquine induced similar effects on dextran (F) when compared to control (E). Scale bar represents 10 μm.

AChE synthesis, an effect that was accompanied by elevated lysosomal pH [13]. Here we have found that Aβ-exposure also affected the fate of internalized surface AChE and did so without disturbing the insertion of newly synthesized AChE into the surface membrane. Aβ-induced changes in the fate of AChE were heralded by an increase in FASII fluorescence, presumably AChE-bound, in LAMP-1 positive late endosomes/early lysosomes, and by a shift from juxtanuclear to peripheral locations. Aβ-exposure also greatly enhanced the accumulation of internalized dextran, a marker of pinocytosis, but it had no effect on the uptake and cellular distribution of Trf or CTB. Altogether, these data point to a selective disturbance of pinocytosis and of intracellular processing of surface-anchored AChE in a fashion that leads to increased cytoplasmic deposits of internalized material.

In this study we showed that FasII not only labels surface AChE but also serves as a probe for the dynamics of AChE internalization and disposal. To the best of our knowledge, this is the first use of FasII to follow the "outside-in" processing of surface enzyme. FasII is recognized as a highly specific ligand for AChE [14], and our data confirm that FasII binding to N1E.115 cells is not only saturable but also fully competed by the selective AChE inhibitor, BW284c51. However, to interpret the FasII observations we must consider the possibility that this ligand could detach from its binding partner at some point and then relocalize inside the cell. Spurious relocalization of free FasII cannot be ruled out completely, but it appears unlikely. One reason is that persistent AChE inhibition was detected even at pH 4, which implies that FasII-AChE complexes are stable even in the acid environment of the mature lysosome. A second reason is that the lysosomal membrane should prevent the escape of free FasII as well as free AChE. Nonetheless, additional studies are warranted to prove that these two proteins remain firmly bound in the membranous compartment revealed here as punctate accumulations of FasII fluorescence.

A straightforward interpretation of the present data is that Aβ-exposure disturbs the intracellular processing of AChE. Increasing amounts of intracellular FasII were observed in

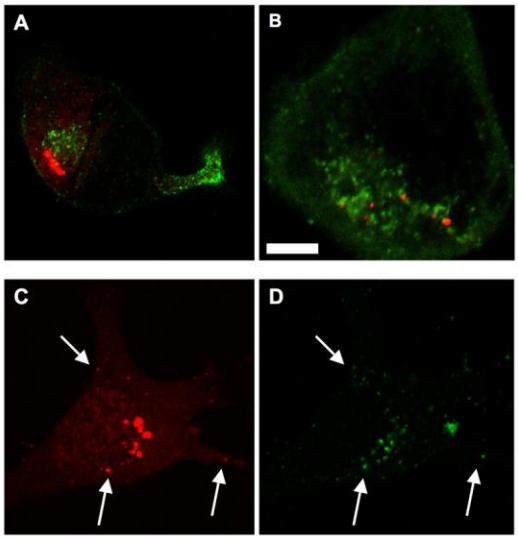

Figure 6. FasII colocalization with markers of known endocytic pathways. A: Internalized FasII (red) and CTB (green). B: Internalized FasII (red) and Trf (green). C, D: Internalized FasII (red) and dextran (green). Arrows indicate structures positive for both FasII and dextran. Scale bars represent 10 μm.

cells labeled with FasII just before Aβ-treatment, and numerous small "salt-and-pepper" deposits of FasII were evident in cells labeled during a prolonged Aβ-exposure. The second phenomenon probably requires lengthy exposure. This effect may reflect toxicity from intracellular Aβ fibrils, or an interruption in trafficking due to accumulation of mal-processed proteins in endosomes secondary to the Aβ-induced elevation in lysosomal pH.

In tests of pinocytosis, both Aβ and chloroquine increased the intracellular accumulation of dextran. These agents share an ability to disturb lysosomal function [13, 21]. Hence, the increased dextran accumulation may be simply another manifestation of Aβ-induced dysfunction in the endosomal-lysosomal compartment. However, because dextran has an α-1,6-polyglucose linkage that resists most cellular glycosidases, dextran accumulation may not depend strongly on lysosomal activity [22]. In that case, the increased dextran level might be taken as a sign of enhanced pinocytosis. In fact, others have postulated a general endocytic upregulation in AD brains [5, 23]. In view of the dissociation that we saw between FasII and dextran label, enhanced pinocytosis may or may not affect AChE processing. In either event, concurrent deficits in lysosomal degradation remain possible. Such a "two-hit effect" was previously shown for β-very low density lipoprotein (β-VLDL), a peptide known to interact directly with Aβ [24] as AChE is suspected of doing [10]. Therefore we cannot exclude the possibility that the scattered cytoplasmic FasII inclusions in Aβ-treated N1E.115 cells reflected both an arrested endosomal processing and an accelerated internalization. An equally plausible explanation would be an Aβ-induced change in a common regulator of pinocytosis and AChE internalization such as the Rho family of GTPases [25].

In addressing the many remaining questions about the normal internalization of surface AChE and the influence of Aβ, alternative pathways of endocytosis must be considered. One such is the CD44/CD43/ICAM-2/ICAM-3 pathway. The CD44 family of proteins share sequence homology in their cytoplasmic tails, which interact with ezrin/radixin/moeisin (ERM) proteins during their internalization [26, 27]. Interestingly, we identified a putative ERM-interacting domain in the sequence of the AChE partner, Proline-Rich Membrane Anchor (PRiMA), located on the cytoplasmic tail (**Figure 7**). This domain makes the AChE-PRiMA complex a candidate substrate for CD44-ERM endocytosis. Another novel possibility to consider, suggested by the minor but reproducible overlap between the localization of dextran and FasII, is that pinocytosis and AChE processing share an intermediate endosome. Dextran appears to share such a structure with APP [28], whose internalization is mediated by caveolae [29, 30]. Because interaction between Aβ and AChE is most robust under acidic conditions, the identity of intermediate compartments is of great interest. One candidate is the Rab5-enriched endosome which has been found to be enlarged in AD [5]. Dysfunction in this pathway could explain the Aβ-induced increases in the surface density of muscarinic receptors that we and others have noted [13, 31-33]. Further characterization of FasII labeled organelles, and tests of co-localization with Rab-5, may therefore be important steps in identifying sites of intracellular Aβ-toxicity.

Figure 7. Amino acid sequence comparison of PRiMA with the CD-44 family of proteins. There are no specific sequence homologies, but two motifs thought to be important in the binding to ERM proteins are shown: runs of positively charged amino acids (labeled in blue) and serine-rich sequences (boxed).

Besides endosomal-lysosomal dysfunction, abnormalities of non-lysosomal protein degradation have been found in neurodegenerative diseases, including AD, and, especially Parkinson's disease (PD). Interestingly, one study of endocytosis in familial PD observed scattered cytoplasmic inclusion bodies similar to those in our Aβ-treated neuroblastoma cells [34]. More effort is needed to elucidate how the Aβ-induced endocytic changes fit into the existing models of AD progression, and how extracellular modification of surface peptides could affect intracellular pathology. Meanwhile, the endosomal-lysosomal pathway represents a potentially relevant and accessible target for therapeutic intervention.

Please address correspondence to: Stephen Brimijoin, Mayo Clinic, 200 First Street SW, Rochester, MN, 55905, Phone (507)-284-8165, Fax (507)-284-9111, E-mail: brimijoi@mayo.edu

References

[1] Glenner GG and Wong CW. Alzheimer's disease: initial report of the purification and characterization of a novel cerebrovascular amyloid protein. Biochem. Biophys. Res. Comm. 1984; 120: 885-890.

[2] Yuan J and Yankner BA. Apoptosis in the nervous system. Nature 2000; 407: 802-809.

[3] Yang AJ, Chandswangbhuvana D, Margol L and Glabe CG. Loss of endosomal/lysosomal membrane impermeability is an early event in amyloid Abeta1-42 pathogenesis. J. Neurosci. Res. 1998; 52: 691-698.

[4] Cataldo A, Rebeck GW, Ghetri B, Hulette C, Lippa C, Van Broeckhoven C, van Duijn C, Cras P, Bogdanovic N, Bird T, Peterhoff C and Nixon RA. Endocytic disturbances distinguish among subtypes of Alzheimer's disease and related disorders. Ann Neurol 2001; 50: 661-665.

[5] Cataldo A, Barnett JL, Pieroni C and Nixon RA. Increased neuronal endocytosis and protease delivery to early endosomes in sporadic Alzheimer's disease: neuropathologic evidence for a mechanism of increased b-amyloidogenesis. J. Neurosci. 1997; 17: 6142-6151.

[6] Liu Y and Schubert D. Cytotoxic amyloid peptides inhibit cellular 3-(4,5-dimethylthiazol-2-yl)-2,5-diphenyltetrazolium bromide (MTT) reduction by enhancing MTT formazan exocytosis. J. Neurochem. 1997; 69: 2285-2293.

[7] Troncoso JC, Cataldo AM, Nixon RA, Barnett JL, Lee M, Checler F, Fowler D, Smialek J, Crain B, Martin L and Kawas C. Neuropathology of preclinical and clinical late-onset Alzheimer's disease. Ann. Neurol. 1998; 43: 673-676.

[8] Castro A and Martinez A. Peripheral and dual binding site acetylcholinesterase inhibitors: implications in treatment of Alzheimer's disease. Mini Rev Med Chem 2001; 1: 267-272.

[9] Ji ZS, Miranda RD, Newhouse YM, Weisgraber

KH, Huang Y and Mahley RW. Apolipoprotein E4 potentiates amyloid beta peptide-induced lysosomal leakage and apoptosis in neuronal cells. J. Biol. Chem. 2002; 277: 21821-21828.
[10] Inestrosa NC, Alvarez A, Perez CA, Moreno RD, Vicente M, Linker C, Casanueva OI, Soto C and Garrido J. Acetylcholinesterase accelerates assembly of amyloid-b-peptides into Alzheimer's fibrils: possible role of the peripheral site of the enzyme. Neuron 1996; 16: 881-891.
[11] Alvarez A, Alarcon R, Opazo C, Campos EO, Munoz FJ, Calderon FH, Dajas F, Gentry MK, Doctor BP, DeMello FG and Inestrosa NC. Stable complexes involving acetylcholinesterase and amyloid-b peptide change the biochemical properties of the enzyme and increase the neurotoxicity of Alzheimer's fibrils. J. Neurosci. 1998; 18: 3213-3223.
[12] Rees T, Hammond PI, Soreq H, Younkin S and Brimijoin S. Acetylcholinesterase promotes beta-amyloid plaques in cerebral cortex. Neurobiol. Aging 2003; 24:777-87.
[13] Hu WT, Gray NW and Brimijoin S. Amyloid-beta increases acetylcholinesterase expression in neuroblastoma cells by reducing enzyme degradation. J. Neurochem. 2003; 86: 470-478.
[14] Bourne Y, Taylor P and Marchot P. Acetylcholinesterase inhibition by fasciculin: crystal structure of the complex. Cell 1995; 83: 503-512.
[15] Peng HB, Xie H, Rossi SG and Rotundo RL. Acetylcholinesterase clustering at the neuromuscular junction involves perlecan and dystroglycan. J. Cell Biol. 1999; 145: 911-921.
[16] Rotundo RL. Acetylcholinesterase biosynthesis and transport in tissue culture. Methods in Enzymology 1983; 96: 353-367.
[17] Johnson CD and Russell RL. A rapid simple radiometric assay for cholinesterase, suitable for multiple determinations. Anal. Biochem. 1975; 64: 229-238.
[18] Henley JR, Krueger EW, Oswald BJ and McNiven MA. Henley JR, Krueger EW, Oswald BJ and McNiven MA (1998) Dynamin-mediated internalization of caveolae. J. Cell Biol. 1998; 141: 85-99.
[19] Rotundo RL and Fambrough DM. Synthesis, transport and fate of acetylcholinesterase in cultured chick embryos muscle cells. Cell 1980; 22: 583-594.
[20] Lazar M, Salmeron E, Vigny M and Massoulié J. Heavy isotope-labeling study of the metabolism of monomeric and tetrameric acetylcholinesteraes forms in the murine neuronal-like T 28 hybrid cell line. J. Biol. Chem. 1984; 259: 3703-3713.
[21] Hoffman KB, Bi X, Pham JT and Lynch G. Beta-amyloid increases cathepsin D levels in hippocampus. Neurosci. Lett. 1998; 250: 75-78.
[22] Ferris AL, Brown JC, Park RD and Storie B. Chinese hamster ovary cell lysosomes rapidly exchange contents. J. Cell Biol. 1987; 105: 2703-2712.
[23] Cataldo A, Peterhoff C, Troncoso JC, Gomez-Isla T, Hyman BT and Nixon RA. Cataldo AM, Peterhoff CM, Troncoso JC, Gomez-Isla T, Hyman BT and Nixon RA (2000) Endocytic pathway abnormalities preced Amyloid b deposition in sporadic Alzheimer's Disease and Down Syndrome. Am. J. Pathol. 2000; 157: 227-286.
[24] Scharnagl H, Tisljar U, Winkler K, Huttinger M, Nauck MA, Grob W, Wieland H, Ohm TG and Marz W. The bA4 amyloid peptide complexes to and enhances the uptake of b-very low density lipoprotein by the low density lipoprotein receptor-related protein and heparan sulfate proteoglycans pathway. Lab. Invest. 1999; 79: 1271-1286.
[25] Ellis S and Mellor H. Regulation of endocytic traffick by Rho family GTPase. Trends Cell Biol. 2000; 10: 85-88.
[26] Yonemura S, Hirao M, Doi Y, Takahashi N, Kondo T, Tsukita S and Tsukita S. Ezrin/Radixin/Moesin (ERM) proteins bind to a positively charged amino acid cluster in the juxtramembrane cytoplasmic domain of CD44, CD43, and ICAM-2. J. Cell Biol. 1998; 140: 885-895.
[27] Serrador JM, Vicente-Manzanares M, Calvo J, Barreiro O, Montoya MC, Schwartz-Albiez R, Furthmayr H, Lozano F and Sanchez-Madrid F. A novel serine-rich motif in the intracellular adhesion molecule 3 is critical for its ezrin/radixin/moesin-directed subcellular targeting. J. Biol. Chem. 2002; 277: 10400-10409.
[28] Yamazaki T, Selkoe DJ and Koo EH. Trafficking of cell surface b-amyloid precursor protein: retrograde and transcytotic transport in cultured neurons. J. Cell Biol. 1995; 129: 431-442.
[29] Bouillot C, Prochiantz A, Rougon G and Allinquant B. Axonal amyloid precursor protein expressed by neurons in vitro is present in a membrane fraction with caveolae-like properties. J. Biol. Chem. 1996; 271: 7640-7644.
[30] Ikezu T, Trapp BD, Song KS, Schlegel A, Lisanti MP and Okamoto T. Caveolae, plasma membrane microdomains for a-secretase-mediated processing of the amyloid precursor protein. J. Biol. Chem. 1998; 273: 10485-10495.
[31] Vogler O, Bogatkewitsch GS, Wriske C, Krummenerl P, Jakobs KH and Van Koppen CJ. Receptor subtype-specific regulation of muscarinic acetylcholine receptor sequestration by dynamin. J. Biol. Chem. 1998; 273: 12155-12160.
[32] Roseberry AG and Hosey MM. Internalization of the M2 muscarinic acetylcholine receptor

proceeds through an atypical pathway in HEK293 cells that is independent of clathrin and caveolae. J. Cell Sci. 2001; 114: 739-746.

[33] Delaney KA, Murph MM, Brown LM and Radhakrishna H. Transfer of M2-muscarinic acetylcholine receptors to clathrin-derived early endosomes following clathrin-independent endocytosis. J. Biol. Chem. 2002; 277: 33439-33446.

[34] Lee HJ and Lee SJ. Characterization of cytoplasmic alpha-synuclein aggregates. Fibril formation is tightly linked to the inclusion-forming process in cells. J. Biol. Chem. 2003; 277: 48976-48983.